JOURNAL OF NATURAL PRODUCTS

Article

pubs.acs.org/jnp

Teucrium polium Phenylethanol and Iridoid Glycoside Characterization and Flavonoid Inhibition of Biofilm-Forming *Staphylococcus aureus*

Wael A. Elmasri,[†] Tianjiao Yang,[†] Phat Tran,[‡] Mohamed-Elamir F. Hegazy,[§] Abdul N. Hamood,[⊥] Yehia Mechref,[†] and Paul W. Paré*[,†]

[†]Department of Chemistry and Biochemistry, Texas Tech University, Lubbock, Texas 79409, United States

[‡]Department of Ophthalmology and Visual Sciences, Texas Tech Health Sciences Center, Lubbock, Texas 79430, United States

[§]Chemistry of Medicinal Plants Department, Center of Excellence for Advanced Sciences, National Research Centre, Giza, 12622, Egypt

[⊥]Department of Microbiology and Immunology, Texas Tech Health Sciences Center, Lubbock, Texas 79430, United States

Supporting Information

ABSTRACT: The chemical composition and biofilm regulation of 15 metabolites from *Teucrium polium* are reported. Compounds were isolated from a CH_2Cl_2–MeOH extract of the aerial parts of the plant and included iridoid and phenylethanol glycosides and a monoterpenoid, together with nine known compounds. The structures were elucidated based on standard spectroscopic (UV, ^1H and ^{13}C NMR), 2D NMR (^1H–^1H COSY, HMQC, HMBC, and NOESY), and/or LC-ESIMS/MS data analyses. Inhibition of the biofilm-forming strain *Staphylococcus aureus* was observed with exposure to compounds **7** and **8**.

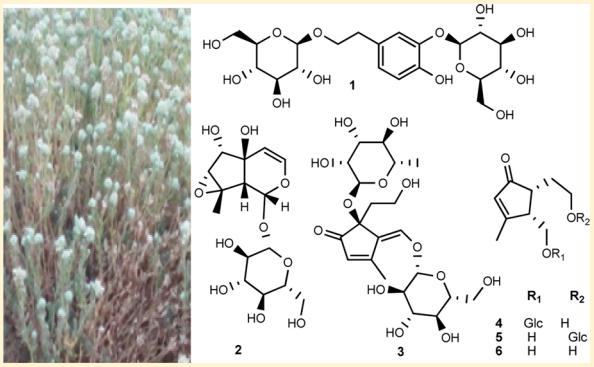

Antimicrobial metabolites have been identified from traditional herbs of the Lamiaceae family that grow in the Mediterranean region including oregano, sage, and thyme.[1] *Teucrium,* a member of the Lamiaceae family, is rich in iridoids and polyphenol metabolites.[2−5] Certain terpenoids of this genus are biologically active as insect antifeedants.[3,4] *Teucrium* has antiseptic properties and is used in the treatment of parasitic diseases such as amoebiasis.[5] Plant extracts of *Teucrium* species also have therapeutic efficacy as antibacterial[6] and anticancer agents.[7] From *Teucrium polium* L., phenylpropanoid and iridoid glycosides as well as flavonoids have been characterized.[8] In the Middle East and Northern Africa, *T. polium* is used for wound healing[9] and specifically has antibacterial activity.[10,11]

Antibacterial activity can be compromised by a variety of bacterial defense mechanisms including enzymatic deactivation of antibiotic molecules and biofilm formation. *Staphylococcus aureus* is a pathogenic bacterium that forms such a biofilm defense and, as a result, is difficult to control.[12] The biofilm serves as a physical barrier that prevent drug penetration.[13] Specifically, biofilms are a structured community of bacteria enclosed in a self-produced extracellular polymer matrix.[14] Bacterial biofilms proceed via three sequential steps: adhesion, proliferation, and detachment. Bacteria first attach to a biotic or abiotic surface. Particularly, *Staph. aureus* can attach to indwelling medical devices with an extraordinary capacity.[15] The attachment is either through direct interaction with the polymer surface of the device or indirectly by connecting to human proteins that initially cover medical devices such as catheters. In the detachment stage, cells diffuse and attach to new infection sites.[15] This detachment can be especially problematic in hospitals, causing nosocomial catheter-related bloodstream infections (CRBSIS). In the United States, CRBSIS treatment costs are estimated upward of $5 billion with mortality rates as high as 36%.[16]

Since *Staph. aureus* can form microcolonies and a biofilm as soon as 5 and 8 h after surface adherence,[17] respectively, early intervention to inhibit bacterial colonization is critical.[18] By preventing initial adhesion, subsequent development of bacterial biofilms that requires orders of magnitude higher minimal bactericidal concentration than the planktonic state will also be prevented.[17] With medical devices such as catheters serving as a common substrate for infectious bacterial colonization, the critical need of antimicrobial agents such as chlorhexidine-silver sulfadiazine to coat and prevent biofilm formation is evident.[16] *T. polium*, a plant rich in antibacterial metabolites, is expected to serve as a source of novel drugs for

Received: May 16, 2014
Published: December 19, 2014

coating medical devices and blocking microbial attachment and colonization.[19] Biological activity of inhibiting biofilm formation was monitored for the isolated compounds from *T. polium* using the green fluorescent protein *Staph. aureus* strain AH133. This fluorescent reporter facilitates in situ visualization of *Staph. aureus* biofilm growth including maturation and detachment events.[20]

A series of novel sesquiterpenoids have been isolated from *T. polium*; however, these metabolites did not exhibit anti-*Staph. aureus* activity. Since a phenylpropanoid glycoside, polumoside, and a flavonoid were previously shown to exhibit biofilm inhibition activity,[21] more polar fractions likely rich in similar carbon skeletons with potential biofilm-inhibiting activity were also purified. Chemical characterization was performed in part by the sensitive and efficient technique of mass spectrometry. Tandem MS analysis has been employed for structural elucidation and/or confirmation of natural products including iridoid glycosides (IGs).[22,23] In this study, six new *T. polium* metabolites were characterized by a combination of NMR and MS data analyses, and in the case where isomers could not be separated, characterization was based solely on LC-MS/MS analysis.

RESULTS AND DISCUSSION

T. polium aerial parts were extracted with CH_2Cl_2–MeOH and partitioned using a gradient of *n*-hexane, CH_2Cl_2, and MeOH. Compounds from the eluted fractions were purified using a combination of Sephadex LH-20 and silica gel CC as well as RP-HLPC. New compounds **1**–**6** along with nine known metabolites were isolated and characterized.

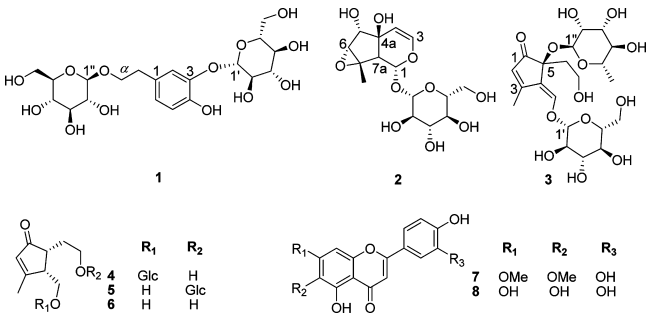

Compound **1** was isolated as a white, amorphous powder with a specific rotation of $[\alpha]_D^{25}$ = −46 (*c* 0.1, MeOH). HRESIMS exhibited a molecular ion $[M + Na]^+$ at *m/z* 501.1580 (calcd 501.1583), which in conjunction with ^{13}C NMR data suggested a molecular formula of $C_{20}H_{30}O_{13}$. The ^1H NMR spectrum displayed an ABX system assigned to a trisubstituted aromatic ring at δ_H 7.00 (d, *J* = 1.8 Hz, H-2), 6.62 (d, *J* = 8.4 Hz, H-5), and 6.68 (td, *J* = 1.4, 2.3, 8.0 Hz, H-6). In addition, an A_2B_2 system was assigned to an ethyl ether unit at δ_H 3.66 (m, H_a-α), 4.04 (m, H_b-α), and 2.72 (t, *J* = 7.3 Hz, H_2-β). Two anomeric signals at δ_H 4.26 (d, *J* = 7.8 Hz, H-1) and 4.88 (d, *J* = 7.3 Hz, H-1) were consistent with a glucose moiety, also observed after acid hydrolysis of **1** via TLC in comparison with an authentic standard. The coupling constants for the anomeric protons at δ_H 4.26 (1H, d, *J* = 7.8 Hz) and 4.88 (1H, d, *J* = 7.3 Hz) were consistent with literature values for a *trans*-diaxial H-1 and H-2 arrangement assigned as β-glucose.[24,25] Acid hydrolysis afforded D-glucose based on GC analysis.

^1H and ^{13}C NMR data were consistent with two β-D-glucose residues (Table 1). HMBC correlations between H-1′ and C-3 and H-1″ and α-C together with NOESY correlations between H-1′ and H_a-α supported the linkage of the glucose units to C-3 and α-C of the phenethyl moiety (Figure 1). These data indicate a compound similar to a known monosaccharide[26] except for an additional β-D-glucose linked to C-3 of the phenethyl moiety. On the basis of these data, the structure was identified as a new natural product, 3-(*O*-β-D-glucopyranosyl)-α-(*O*-β-D-glucopyranosyl)-4-hydroxyphenylethanol.

Compound **2** was isolated as a yellow, amorphous powder, with a specific rotation of $[\alpha]_D^{25}$ = −12 (*c* 0.2, MeOH). HRESIMS data exhibited a molecular ion $[M + Na]^+$ at *m/z* 385.1110 (calcd 385.1110), which in conjunction with ^{13}C NMR data suggested a molecular formula of $C_{15}H_{22}O_{10}$. On the basis of ^1H and ^{13}C (Table 1) as well as 2D NMR data (Figure 1), **2** is an 11-nor-iridoid similar to 7,8-*epi*-antirrinoside[27] except for the configurations at C-1 and C-5. NOE correlations between H-5 and H_3-8 established an α-OH group at C-5, while correlations between H-1 and H-7a established an α-*O*-glucoside moiety at C-1. Acid hydrolysis afforded D-glucose based on GC analysis. The anomeric proton at δ_H 4.64 (1H, d, *J* = 7.8 Hz) established a β-glucose configuration.[24,25] On the basis of these spectroscopic data, the structure was assigned as 1α-(β-D-glucopyranoxy)-6α,7α-epoxy-4aβ,5α-dihydroxy-7-methyl-1,4a,5,6,7,7aβ-hexahydrocyclopenta[*c*]pyran, a new natural product.

Compound **3** was isolated as a white, amorphous powder, with a specific rotation of $[\alpha]_D^{25}$ = 4 (*c* 0.5, MeOH). The HRESIMS data exhibited a molecular ion $[M]^+$ at *m/z* 493.1924 (calcd 493.1921) and $[M + Na]^+$ at *m/z* 515.1743 (calcd 515.1740), which in conjunction with ^{13}C NMR data suggested a molecular formula of $C_{21}H_{32}O_{13}$. An HRESIMS/MS of *m/z* 515.1743 produced ions at *m/z* 497.0902 $[M + Na - H_2O]^+$, 369.0877 $[M + Na - Rha]^+$, and 353.1708 $[M + Na - Glc]^+$. ^1H and ^{13}C NMR data (Table 1) exhibited signals assignable to two methyl groups at δ_H 2.18 (s, H_3-10) and 1.03 (d, H_3-6″), two methylenes at δ_H 3.52 (m, H_2-8, oxygenated) and 2.17 (m, H_2-9), an exocyclic double bond at δ_C 145.6 and 121.8, an endocyclic double bond at δ_C 127.2 and 171.2, two anomeric protons at δ_H 4.74 (d, *J* = 7.3 Hz, H-1′) and 4.71 (d, *J* = 1.4 Hz, H-1″), and a carbonyl group at δ_C 206.9. On the basis of 1D and 2D NMR data for the known iridoid derivatives,[28,29] and the fact that the formula of **3** possessed 2 mass units more than teucardoside,[21] **3** was proposed to be a seco-iridoid, formed by cleavage of the C-6—O-7 bond. HMBC data were consistent with this proposed structure with correlations within the ring structure observed between the methyl protons at δ_H 2.18 and signals at δ_C 127.2 (C-2), 171.2 (C-3), and 121.8 (C-4); the carbon chemical shifts of C-2 and C-3 were consistent with an endocyclic double bond.[28] HMBC correlations were also observed between H-2 (δ_H 5.8) and signals at δ_C 206.9 (C-1), 81.7 (C-5), and C-4. HMBC signals for the acyclic portion were also consistent with the proposed structure, as correlations from H-6 (δ_H 7.06) to C-3 and C-5 were observed, allowing for the assignment of C-6. Moreover, HMBC correlations from H_2-8 (δ_H 3.52) to C-5 and from H_2-9 (δ_H 2.17) to C-1 and C-4 allowed for the assignment of C-8 and C-9, respectively. In addition, HMBC correlations were used to assign the positions of two sugar units with correlations observed between H-1′ (δ_H 4.74) and C-6 as well as between H-1″ (δ_H 4.71) and C-5. Acid hydrolysis afforded D-glucose and L-rhamnose based on GC analysis. Beta- and α-configurations were established for glucose and rhamnose, respectively, based on anomeric proton coupling constants.[24,25] An absence of HMBC correlations between H_2-8 and C-6 and/or between H-

dx.doi.org/10.1021/np5004092 | J. Nat. Prod. 2015, 78, 2–9

Table 1. $^{1}H/^{13}C$ NMR Spectroscopic Data for Compounds 1−3 (δ in ppm, J in Hz) (400 MHz, Methanol-d_4)[a]

	1		2		3[b]	
position	δ_H (J in Hz)	δ_C	δ_H (J in Hz)	δ_C	δ_H (J in Hz)	δ_C
1		131.7	5.37 d (5.5)	95.1		206.9
2	7.00 d (1.8)	119.4			5.8 s	127.2
3		146.6	6.35 d (5.5)	143.0		171.2
4		146.7	4.90 d (6.4)	107.6		121.8
4a				74.7		
5	6.62 d (8.2)	125.1	3.90 brs	78.5		81.7
6	6.68 td (1.4, 2.3)	116.8	3.36 m	66.2	7.06 s	145.6
7	2.72 t (7.3)	36.5		64.2		
7a			2.35 d (6.4)	53.2		
8	3.66 m	71.7	1.42 s	17.6	3.52 m	58.6
	4.04 m					
9					2.17 m	39.0
10					2.18 s	14.7
	Glucose		Glucose		Glucose	
1′	4.26 d (7.8)	104.3	4.64 d (7.8)	99.6	4.74 d (7.3)	105.7
2′	3.18	75.1	3.19	74.7	3.30	74.6
3′	3.45	77.6	3.35	77.7	3.39	77.8
4′	3.26	71.6	3.25	71.8	3.66	72.3
5′	3.41	78.3	3.21	78.3	3.33	78.3
6′	3.65 m	62.5	3.61	62.6	3.78	61.7
	3.87 td (2.3)		3.87 td		3.83	
	Glucose				Rhamnose	
1″	4.88 d (7.3)	104.2			4.71 d (1.4)	97.7
2″	3.46	74.9			3.81	72.6
3″	3.25	77.9			3.40	70.5
4″	3.38	71.5			3.28	73.9
5″	3.33	78.0			3.62	70.7
6″	3.67	62.8			1.03 d (6.5)	17.61
	3.85 td (2.3)					

[a]Overlapped signals are reported without designating multiplicity. [b]Oxymethylene (C-6), hydroxyethyl [C-9 ($-CH_2$) and C-8 ($-CH_2OH$)], and methyl (C-10).

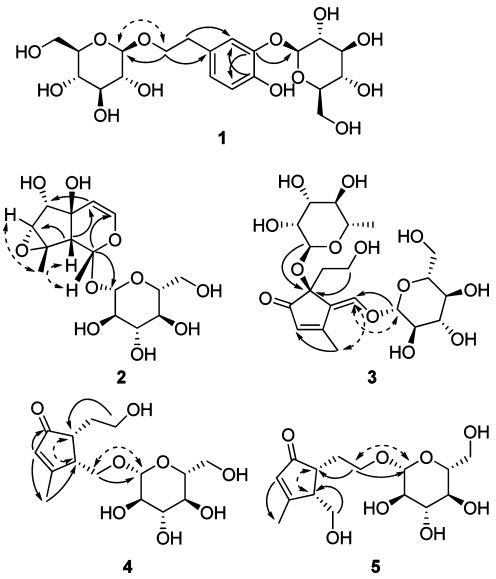

Figure 1. HMBC (solid arrow) and NOE (hashed, double-headed arrow) correlations observed for 1−5.

6 and C-8 were also consistent with a seco-iridoid structure. On the basis of biogenetic precedent[3−5] and characterized routes for iridoid biosynthesis,[30] the *O*-rhamnopyranosyl moiety at C-5 was assigned a β-configuration (Figure 1), although direct chemical data to confirm this configurational assignment have not been obtained. On the basis of these data, the structure was assigned as 4-[(β-D-glucopyranosyloxy)methylene]-5α-(2-hydroxyethyl)-5-(α-L-rhamnopyranosyloxy)-3-methylcyclopent-2-en-1-one, a new natural product.

Compound **4** was isolated as a mixture with compound **5**. The two isomers formed a yellow, amorphous powder, with a specific rotation of $[\alpha]_D^{25} = -29$ (c 0.2, MeOH). HRESIMS exhibited a molecular ion $[M^+]$ at m/z 333.1549 (calcd 333.1549) and $[M + Na]^+$ at m/z 355.1366 (calcd 355.1368), which in conjunction with ^{13}C NMR data suggested a molecular formula of $C_{15}H_{24}O_8$. ^{1}H and ^{13}C NMR data for **4** (Table 2) showed signals assignable to a methyl group at δ_H 2.14 (s, H_3-10) and four methylenes at δ_H 3.75 and 4.02 (both m, H_2-6), 3.8 (d, H_2-8), 1.56 and 2.07 (both m, H_2-9), and 3.62 and 3.83 (both m, H_2-6′). In addition, an anomeric proton at δ_H 4.23 (d, J = 8.7 Hz, H-1′), a carbonyl at δ_C 214.3, and an olefinic proton at δ_H 5.91 (s, H-2) with two olefinic signals at δ_C 131.5 and 182.3 were observed. On the basis of 1D and 2D NMR data as well as comparison with **3** and teuhircoside, a known monoglucoside iridoid derivative,[28] **4** was proposed to be a seco-iridoid similar to **3** except for the absence of a 5-*O*-rhamnopyranosyl moiety and saturation of the exocyclic double bond. This similarity allowed for assignment of all proton and carbon signals. The anomeric proton coupling constant established a β-glucose configuration.[24,25] Acid hydrolysis of **4** afforded D-glucose based on GC analysis. Assignment of the

dx.doi.org/10.1021/np5004092 | J. Nat. Prod. 2015, 78, 2−9

Table 2. $^{1}H/^{13}C$ NMR Spectroscopic Data for Compounds 4–6 (δ in ppm, J in Hz) (400 MHz, Methanol-d_4)[a]

	4		5		6	
position	δ_H (J in Hz)	δ_C	δ_H (J in Hz)	δ_C	δ_H (J in Hz)	δ_C[b]
1		214.3		213.9		
2	5.91 s	131.5	5.89 s	131.2	5.93 s	131.5
3		182.3		181.8		
4	2.75 brs	54.9	2.84 brs	52.9	2.72 brs	55.0
5	2.49 m	47.8	2.52 m	48.2	2.39 m	48.1
6	3.75 m	62.1	3.68 m	69.9	3.70 m	61.4
	4.02 m					
8	3.8 d (4.1)	68.8	3.75 m	61.1	3.87 t (6.8)	61.2
			4.10 m			
9	1.56 m	32.1	1.61 m	34.5	1.59 m	
	2.07 m		1.94 m		1.96 m	
10	2.14 s	17.7	2.16 s	17.8	2.16 s	
	Glucose		Glucose			
1′	4.23 d (8.7)	104.4	4.27 d (8.2)	104.3		
2′	3.13 m	75.1	3.13 m	74.9		
3′	3.24	78.0	3.24	78.0		
4′	3.24	71.5	3.32	71.6		
5′	3.24	78.1	3.24	78.0		
6″	3.62	62.7	3.62	62.7		
	3.83 brd (11.9)		3.83 brd (11.9)			

[a]Multiplicity; hydroxy- or oxymethyl (C-6), hydroxy- (R = H) or oxyethyl (R = Glc) [C-9 ($-CH_2$) and C-8 ($-CH_2OR$)], and methyl (C-10). [b]Partially unclear ^{13}C signals with overlapped signals reported without designating.

relative configuration at C-4 and C-5 was based on literature data and an NOE correlation between H-4 and H-5 (Figure 1). Therefore, the structure was assigned as 4α-[(β-D-glucopyranosyloxy)methyl]-5α-(2-hydroxyethyl)-3-methylcyclopent-2-en-1-one, a new natural product.

The ^{1}H and ^{13}C NMR data (Table 2) of compound **5** exhibited signals assignable to a methyl group at δ_H 2.16 (s, H_3-10) as well as four methylenes at δ_H 3.68 (d, H_2-6), 3.75 and 4.10 (both m, H_2-8), 1.61 and 1.94 (both m, H_2-9), and 3.62 and 3.83 (both m, H_2-6′). In addition, an anomeric proton at δ_H 4.27 (d, J = 8.7 Hz, H-1′), a carbonyl at δ_C 213.9, and an olefinic proton at δ_H 5.89 (s, H-2) with two olefinic signals at δ_C 131.2 and 181.8 were observed. Comparison of 1D and 2D NMR data for **5** with those of **4** indicated similar compounds except for the site of glucosylation being shifted to C-6 in **4** to C-8 in **5**. Therefore, the structure was assigned as 5α-[2-(β-D-glucopyranosyloxy)ethyl]-4α-hydroxymethyl-3-methylcyclopent-2-en-1-one, a new natural product.

MS/MS data for the aglycone of **4** and **5** were consistent with the above structural assignments; shared fragments included ions at m/z values of 171, 153, and 135, corresponding to a loss of a glucopyranosyl moiety as well as one and two water molecules,[31] respectively (Figure 2). Since both **4** and **5** contain the same aglycone product, unambiguous MS/MS assignment was not necessary. The two regioisomers exhibited differences in fragment-ion intensities (Table 3), as has been observed with analogous compounds.[32] Additionally, aglycone MS/MS data showed identical ion peaks within acceptable experimental error.

Compound **6** was isolated as a pale yellow, amorphous powder. The HRESIMS/MS exhibited a precursor ion $[M + Na]^+$ at m/z 193.0837 (calcd 193.0840) and $[M + H]^+$ at m/z

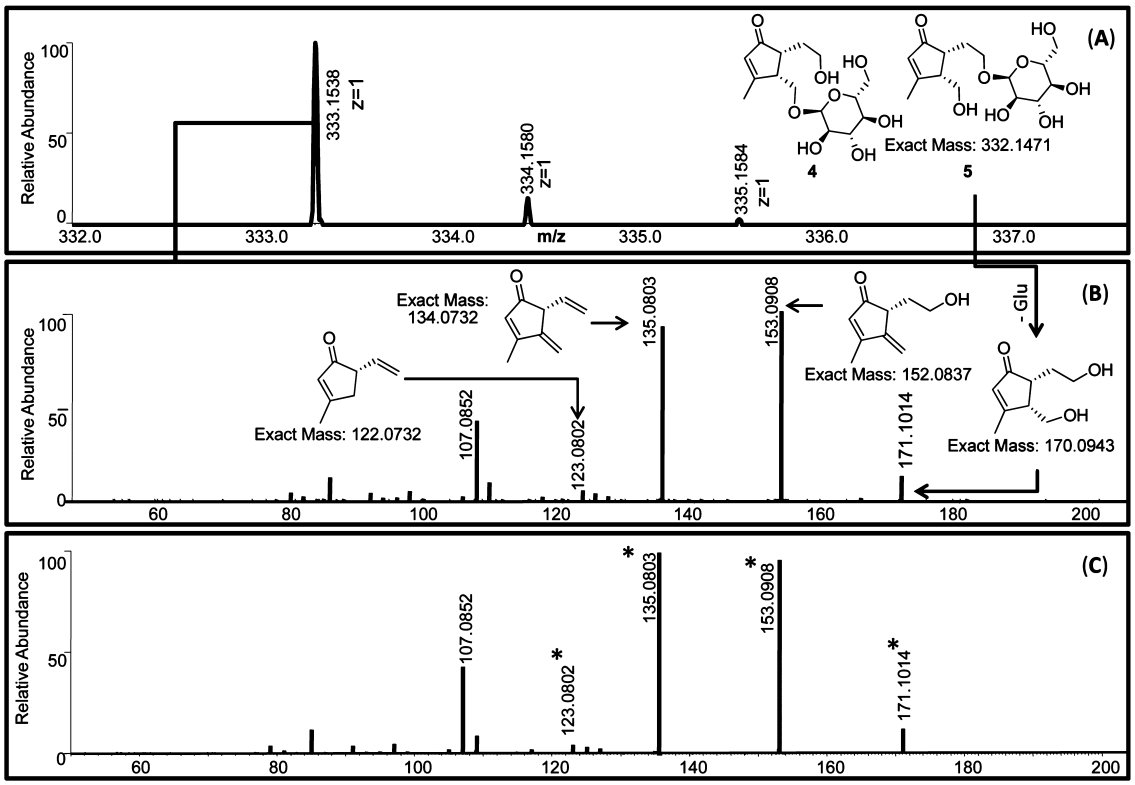

Figure 2. (A) Mass spectrum of **4** or **5**, (B) tandem mass spectrum of **4** or **5**, and (C) tandem mass spectrum of **6**. An asterisk (*) indicates the alignment of the ion peak with the above spectrum.

dx.doi.org/10.1021/np5004092 | J. Nat. Prod. 2015, 78, 2–9

Table 3. Accurate MS and Elemental Compositions of Main Product Ions for Protonated 4 and 5 by HCD-MS/MS Analysis in Positive-Ion Mode

compound	$[M + H]^+$ (m/z)	fragment ion (m/z)	fragment calculated (m/z)	fragment elemental composition	fragment mass accuracy (ppm)	relative intensity (%)
4 or **5**	333.1538	171.1014	171.1016	$C_9H_{14}O_3$	−1.1	10
(t_R[a] 17.6 min)		153.0909	153.0910	$C_9H_{12}O_2$	−0.6	82
		135.0802	135.0805	C_9H_8O	−2.2	100
		123.0803	123.0805	$C_8H_{10}O$	−1.6	18
5 or **4**	333.1538	171.1014	171.1016	$C_9H_{14}O_3$	−1.1	15
(t_R 18.8 min)		153.0908	153.0910	$C_9H_{12}O_2$	−1.3	100
		135.0803	135.0805	C_9H_8O	−1.4	92
		123.0802	123.0805	$C_8H_{10}O$	−2.4	5

[a]Retention time.

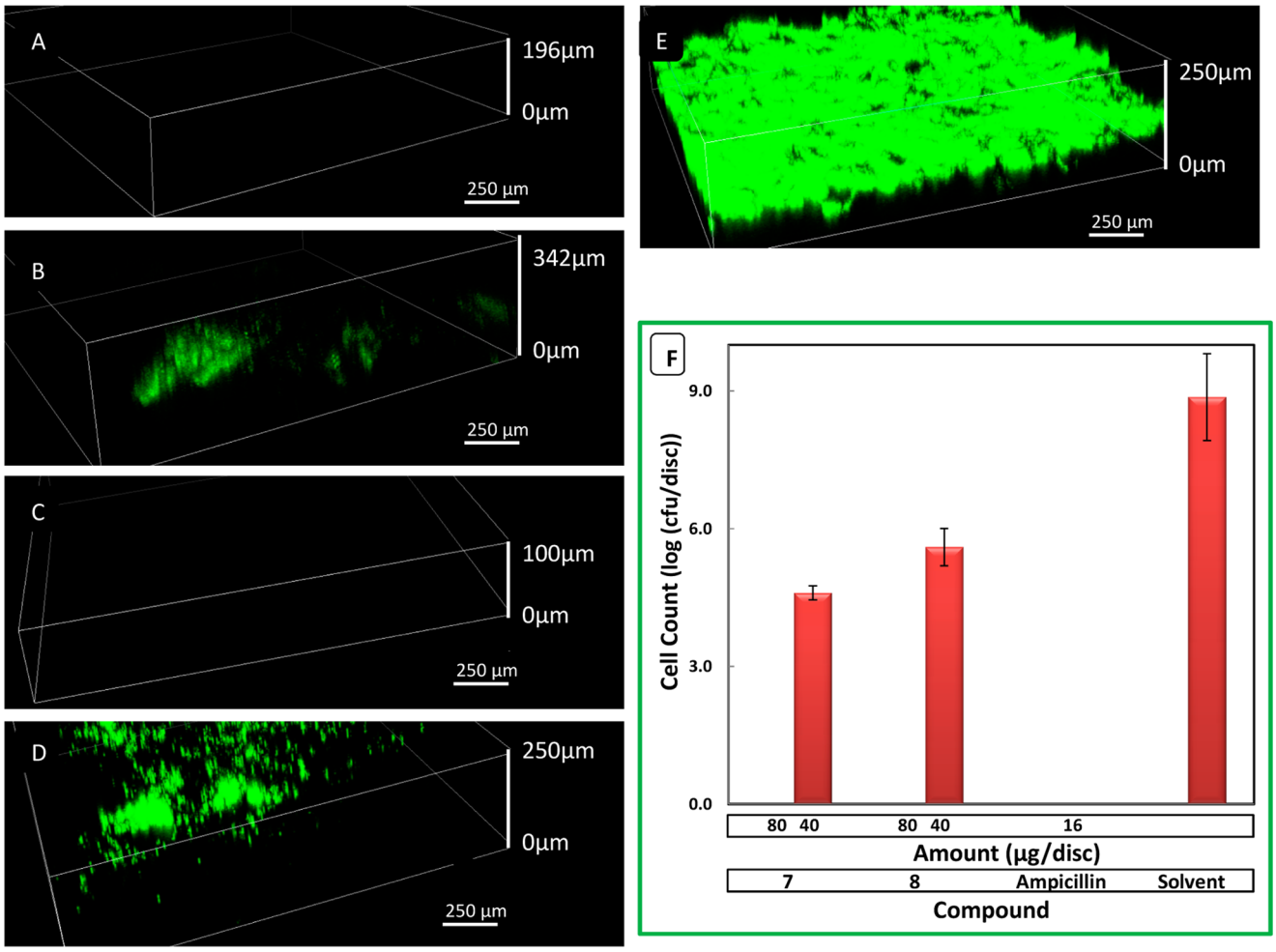

Figure 3. Biofilm prevention in transgenic green fluorescent protein (GFP) *Staph. aureus* with **7** (80 μg) (A), **7** (40 μg) (B), **8** (80 μg) (C), and **8** (40 μg) (D); representative 3D-generated confocal images are shown with DMSO as a solvent control (E). Bacterial colony forming units (CFUs) present in the biofilm with exposure to **7**, **8**, ampicillin, or solvent (F) with values representing the mean ± SD (n = 3).

171.1014 (calcd 171.1021), which in conjunction with ^{13}C NMR data suggested a molecular formula of $C_9H_{14}O_3$. An insufficient amount of **6** was available for complete NMR chemical characterization; however, ^1H NMR combined with equivalent MS/MS fragmentation data between the aglycones of **4** and **5** with **6** allowed for the assignment of **6** as 5α-(2-hydroxyethyl)-4α-hydroxymethyl-3-methylcyclopent-2-en-1-one, also a new natural product.

In addition, nine known compounds, namely, 3′,4′,5-trihydroxy-6,7-dimethoxy-flavone (**7**),[33] 5,6,7,3′,4′-pentahydroxyflavone (**8**),[34] cirsimaritin,[35] luteolin,[36] 3,4-dihydroxy-3-(*O*-β-D-glucopyranosyl)phenethanol,[26,37] 2-(3,4-dihydroxyphenyl)ethanol,[26] (7*S*,8*R*)-4-(*O*-β-D-glucopyranosyl)-dehydrodiconiferyl alcohol,[38] (7*S*,8*R*)-5-methoxy-4-(*O*-β-D-glucopyranosyl)dehydrodiconiferyl alcohol,[39] and teuhircoside,[40] were isolated and identified by spectroscopic comparisons with literature values.

All compounds identified here were screened for their activity against the biofilm-forming *Staphylococcus* strain AH133. AH133 strain, previously transformed with the green

dx.doi.org/10.1021/np5004092 | J. Nat. Prod. 2015, 78, 2−9

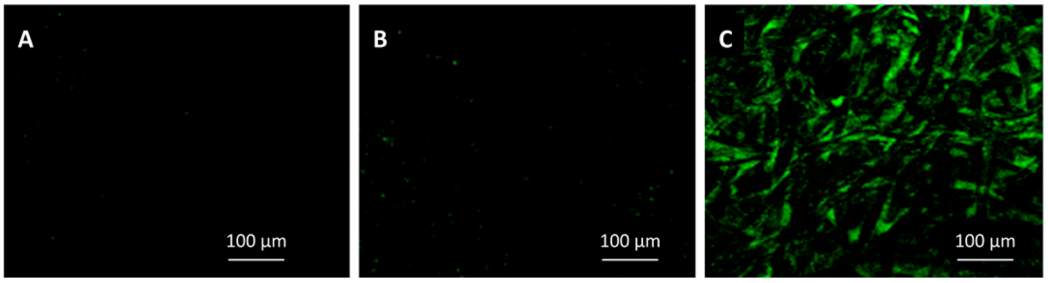

Figure 4. Biofilm elimination of transgenic GFP *Staph. aureus* with **7** (80 μg) (A) and **8** (80 μg) (B) in comparison with a solvent control (DMSO) (C); representative 2D-generated confocal images, exhibiting GFP expression, are shown.

fluorescence protein (GFP) gene marker for facilitating visualization of bacterial growth, was used. In the zone of inhibition assay, activity against planktonic bacteria (free-living nonbiofilm cells) was evaluated. Compounds **7** and **8** produced a clear zone of inhibition of 10.3 mm (SD = ±0.58) and 8.0 mm (SD = ±0.06), respectively, at 16 mg/mL. In the biofilm prevention assay, a cellulose disc served as a site of bacterial attachment.[19,41] During the biofilm development, the ability of compounds to inhibit AH133 growth was compared to a commercially used, broad-spectrum inhibitor of bacterial cell-wall formation, ampicillin. Ampicillin inhibited AH133 at 16 μg/disc, whereas without antibiotic treatment, AH133 produced a thick homogeneous mass associated with biofilm formation (Figure 3E). Compounds **7** and **8** showed no AH133 inhibition at 10 and 20 μg/disc; however, reduced growth at 40 μg/disc (Figure 3B and D) was observed. AH133 growth was completely inhibited at 80 μg/disc (Figure 3A and C). Growth inhibition was confirmed by quantitative analysis via colony counting. Compounds **7** and **8** significantly reduced biofilms on discs treated with 40 μg/disc ($p < 0.01$) compared with solvent controls (Figure 3F). Complete inhibition was observed at 80 μg/disc (Figure 3F). In the biofilm elimination assays, colony forming units (CFUs) were not recovered from discs treated with 80 μg/disc of **7** or **8** (Figure 4). Both **7** and **8** are flavonoids carrying a 3′,4′-dihydroxy B-ring pattern, and **8** possesses a 5,7-dihydroxy group that is reported to confer antibacterial activity.[42] With future cytotoxicity studies of compounds **7** and **8**, the potential use of these metabolites as an antimicrobial biofilm inhibitor for coating medical devices such as catheters can be assessed. Future proteomic studies will probe how these biologically active metabolites from *T. polium* affect biofilm formation and/or other cellular pathways.

EXPERIMENTAL SECTION

General Experimental Procedures. Optical rotations were measured in MeOH on an Autopal IV automatic polarimeter (Rudolph Research Analytical) equipped with a 10 cm microcell and a sodium lamp (λ_{max} = 589 nm). UV data were obtained on a Genesys 20 spectrophotometer. IR (KBr) spectra were recorded on a ThermoNicolet model IR 100 spectrophotometer. NMR spectra were obtained on a Varian (Palo Alto, CA, USA) Unity Inova 500 NMR spectrometer (^{1}H at 500 MHz and ^{13}C at 125 MHz) equipped with VNMR 6.1C software and Sun hardware; chemical shifts were reported in δ (ppm) and J coupling in Hz. The ^{13}C NMR multiplicities were determined by DEPT experiments. NOE measurements were obtained from 2D NOESY experiments. One-bond heteronuclear ^{1}H−^{13}C connectivities were determined by HMQC, and two- and three-bond ^{1}H−^{13}C connectivities were determined by HMBC experimentation. HRESIMS, LC/MS, and LC/MSMS analyses were performed on a Dionex Ultimate 3000 UHPLC system interfaced with an LTQ Orbitrap Velos (Thermo Scientific, Pittsburgh, PA, USA) mass spectrometer. Data were processed using Xcalibur Qual browser software (Thermo Scientific, Pittsburgh, PA, USA). GCMS analysis was performed on an ISQ QD Single Quadrupole GCMS system, and data were processed using Xcalibur software (Thermo Scientific). HPLC was performed using a preparative C_{18} column (21.2 × 250 mm, 10 μm) on an Agilent 1100 apparatus equipped with a Rheodyne injector and with UV detectors. Column chromatography was carried out using EMD silica gel 60 (70−230 mesh). Analytical TLC was performed on EMD silica gel 60 F_{254} sheets, 0.25 mm thick. Confocal laser scanning microscopy (CLSM) images and data files, taken for each 2 μm of biofilm depth, were acquired using an Olympus IX 71 upright microscope with a 20× optical lens and Fluoview software (Olympus America).

Plant Material. Aerial parts of *T. polium* were collected in June 2010 from North Sinai, Egypt, and authenticated by one of the authors, M.E.F.H. A voucher specimen has been deposited in the Herbarium of St. Katherine protectorate, Egypt (voucher ID: SK-105).

Extraction and Isolation. Air-dried aerial plant tissue (2 kg) was crushed. The resulting powder was extracted at room temperature with CH_2Cl_2−MeOH (1:1). The solvent was evaporated, and the residue (210 g) subjected to silica gel CC eluting with *n*-hexanes, CH_2Cl_2, and MeOH in an increasing order of polarity up to 100% MeOH to afford 398 fractions. On the basis of metabolite complexity of chromatographic analysis, fractions 233−293 were further purified for spectroscopic analysis and biological testing.

Similar TLC fractions 233−249 were combined (3.6 g), concentrated in vacuo, redissolved in MeOH, and subjected to silica gel CC. Compounds were eluted with a gradient of CH_2Cl_2−MeOH (50:50) up to 100% MeOH, and fractions were monitored by TLC, eluting with CH_2Cl_2−MeOH−H_2O (2:4:1), to afford 40 subfractions. Pooled fractions 20 and 21 (1 g) were subjected to Sephadex LH-20 gel CC eluted with an isocratic system of CH_2Cl_2−MeOH (25:75). Pooled fractions included 2−18 (A), 21 and 22 (B), 34−40 (C), 40−43 (D), and 44−46 (E). Subfraction A (300 mg) included a mixture of flavonoids; B afforded **7** (6 mg). Subfraction C (450 mg) afforded **8** (3 mg) after additional RP-HPLC purification eluting with an isocratic system of MeOH−H_2O (25:75). Subfractions D and E afforded cirsimaritin (4 mg) and luteolin (5.5 mg), respectively.

Similar TLC fractions 250−265 were recombined (9 g), concentrated in vacuo, and subjected to silica gel CC eluting with a gradient of CH_2Cl_2−MeOH starting with 9:1 up to 0.5:9.5; fractions were monitored by TLC eluting with CH_2Cl_2−MeOH−H_2O (3:5:0.5). Pooled fractions included 3−5 (A′), 6 (B′), and 30−46 (C′). Subfraction A′ (1.5 g) afforded **5** (7 mg), (7*S*,8*R*)-4-(*O*-β-D-glucopyranosyl)dehydrodiconiferyl alcohol (12 mg), and (7*S*,8*R*)-5-methoxy-4-(*O*-β-D-glucopyranosyl)dehydrodiconiferyl alcohol (8.5 mg) by RP-HPLC eluting with an isocratic MeOH−H_2O (35:65) solvent. Subfraction B′ (250 mg) afforded **6** (0.7 mg) by RP-HPLC eluting with an isocratic system of MeOH−H_2O (19:81). Subfraction C′ (3.1 g) was subjected to Sephadex LH-20 gel CC eluted with MeOH; 19 subfractions were obtained. Fractions 6−11 (600 mg) were pooled and subjected to Sephadex LH-20 gel CC eluted with MeOH to afford 22 fractions. Subfractions 5−18 (210 mg) were purified by RP-HPLC eluting with an isocratic system of MeOH−H_2O (17:83;

dx.doi.org/10.1021/np5004092 | J. Nat. Prod. 2015, 78, 2−9

acidified with 0.1% formic acid) to afford **4**/**5** (9 mg) and 2-(3,4-dihydroxyphenyl)ethanol (1.7 mg).

Similar TLC fractions 284−293 were combined (6 g), concentrated in vacuo, and subjected to silica gel CC, eluted with a gradient of CH_2Cl_2−MeOH from 7:2 to 0.1:9.9; fractions were monitored by TLC eluting with CH_2Cl_2−MeOH−H_2O (6:2:0.5). Pooled fractions included 3−6 (A″) and 7−11 (B″). Subfraction A″ (800 mg) was a mixture of inseparable metabolites. Subfraction B″ (650 mg) was pooled and purified by RP-HPLC eluting with a MeOH−H_2O (acidified with 0.1% formic acid) gradient from 41:59 to 50:50 to afford 3,4-dihydroxy-3-(*O*-*β*-D-glucopyranosyl)phenethanol (1.5 mg) and teuhircoside (2.6 mg).

ESIMS Analytical Conditions. A mixture of compounds **4** and **5** was loaded onto a C_{18} cartridge column (2 cm × 75 μm, 3 μm, 100 Å). The separation was achieved using a C_{18} nanocolumn (15 cm × 75 μm, 2 μm, 100 Å) with a flow rate of 0.35 μL/min. The separation was attained using the following elution gradient: initially, 5% mobile phase B was applied for 10 min; the gradient was then increased linearly from 5% B to 40% B over 20 min and then was kept at 40% B for 5 min. From 35 to 40 min, the gradient was dropped linearly from 40% B to 5% B and then kept at 5% B for 5 min. Mobile phase A was 2% MeCN in H_2O with 0.1% HCO_2H, while mobile phase B was 100% MeCN with 0.1% HCO_2H. The positive-ion mode ESIMS data were collected in an *m*/*z* range of 50−800 with a 15 000 resolution FT mass analyzer. The spray voltage was set to 1.5 kV, and the capillary temperature was set to 300 °C. The MS/MS experiment was conducted using a high-energy collision dissociation (HCD) cell with 50% normalized collision energy. Three MS^2 were conducted after each MS scan in a data-dependent acquisition (DDA) mode.

Compound **1**: white amorphous powder; $[\alpha]_D^{25}$ = −46 (*c* 0.1, MeOH); UV (MeOH) λ_{max} 286 nm; IR (KBr) ν_{max} 3320, 3146, 3048, 1654, 1406, 1276, 1073 cm^{-1}; HREIMS *m*/*z* 501.1580 (calcd for $C_{20}H_{30}O_{13}Na$, 501.1583).

Compound **2**: yellow, amorphous powder; $[\alpha]_D^{25}$ = −12 (*c* 0.2, MeOH); UV (MeOH) λ_{max} 283 nm; IR (KBr) ν_{max} 3342, 2892, 1593, 1353, 1276, 1077, 1037, 985. HREIMS *m*/*z* 385.1110 (calcd for $C_{15}H_{22}O_{10}Na$, 385.1110).

Compound **3**: white, amorphous powder; $[\alpha]_D^{25}$ = 4 (*c* 0.5, MeOH); UV (MeOH) λ_{max} 301 nm; IR (KBr) ν_{max} 3287, 2965, 1701, 1686, 1510, 1243, 1067, 1048, 817 cm^{-1}; HREIMS *m*/*z* 493.1924 (calcd for $C_{21}H_{32}O_{13}Na$, 493.1921).

Compounds **4** and **5**: yellow, amorphous powder; $[\alpha]_D^{25}$ = −29 (*c* 0.2, MeOH); UV (MeOH) λ_{max} 286 nm; IR (KBr) ν_{max} 3299, 2923, 2365, 1675, 1617, 1262, 1075, 1039 cm^{-1}; HREIMS *m*/*z* 333.1549 (calcd for $C_{15}H_{24}O_8$, 333.1549) and 355.1366 (calcd for $C_{15}H_{24}O_8Na$, 355.1368).

Acid Hydrolysis of 1−5. A solution of **1**−**5** (1.5 mg/sample) in 2 N HCl (0.5 mL) was heated under reflux for 2 h. After cooling, the reaction mixture was neutralized with Amberlite IRA-68, and the resin was removed by filtration. The filtrate was extracted with EtOAc (2 × 2 mL). The aqueous layer was concentrated, and the sugars were identified using TLC eluting with *n*-hexane−EtOAc−MeOH−HOAc−H_2O (1:4:2:0.5:0.5) by comparison with authentic standards.[43]

Gas Chromatography Analysis. For sugar identification, an aqueous aliquot was trimethylsilylated with *N*-trimethylsilylimidazole (TMSI) for 2 h at room temperature. After addition of distilled H_2O, the mixture was partitioned with *n*-hexane, and the *n*-hexane layer was analyzed by GCMS. For sugar configuration identification, 0.2 mL of L-cysteine methyl ester hydrochloride (0.06 M) in pyridine was added to the aqueous layer concentrate. The mixture was stirred at 60 °C for 1 h; then 0.2 mL of TMSI was added, and the mixture was kept at room temperature for 2 h. The reaction mixture was partitioned with *n*-hexane and distilled H_2O, and the *n*-hexane layer was analyzed by GCMS. The conditions of GCMS were as follows: detector temperature, 250 °C; injection temperature, 290 °C; initial column oven temperature 40 °C, then raised to 260 at 10 °C/min, final temperature maintained for 7 min; carrier, He gas (split ratio, 1:17). For compounds **1**−**5**, D-glucose (retention time 26.18 min) and for **3** L-rhamnose (retention time 24.63 min) were confirmed by comparison with the corresponding derivatized authentic standard.

Screening for Antibacterial Activity. *Staph. aureus* strain AH133-GFP was grown overnight in Luria−Bertani (LB) broth and diluted with phosphate buffer saline (PBS) (2.6 μM KCl, 137 μM NaCl, 1.7 μM KH_2PO_4, and 10 μM Na_2HPO_4 at pH = 7.4) to 0.5 optical density (OD) of ca. 1×10^8 CFUs/mL. A culture aliquot was spread onto an LB agar plate. Sterile cellulose discs, containing three different concentrations from each test compound, were placed onto inoculated plates. Plates were incubated at 37 °C for 18−24 h, following which the zone of inhibition (clear zone) was measured.

AH133-GFP Biofilm Regulation. *Staph. aureus* AH133-GFP was grown overnight in LB broth and diluted with PBS to 0.5 OD. The cultures were serially diluted 10-fold to obtain inoculums of ca. 1×10^5 CFUs/mL, and the tested compounds were prepared at concentrations of 10, 20, 40, 80, and 160 μg/10 μL of solvent, DMSO. In the biofilm prevention assay, 10 μL of diluted culture was applied to a 6 mm cellulose disc (Becton Dickinson) and incubated for 5 min at room temperature, and 10 μL of the test compound, DMSO, and/or ampicillin (triplicates of each concentration) was added. Plates were incubated for 24 h at 37 °C. In the biofilm elimination assay, an aliquot (10 μL) of the diluted culture was applied to each disc, and plates were incubated at room temperature for 8 h; an aliquot (10 μL) of either DMSO or *T. polium* test compounds (triplicates of each concentration) was added to each disc, and plates were incubated at 37 °C for 24 h. For both assays, biofilms were imaged via CLSM. The biofilm was quantified by counting CFUs per disc.[41] The cellulose discs were removed from the LB plates, and biofilm was disrupted by vortexing in 1 mL of PBS. The serially diluted bacterial suspension was spotted onto LB agar plates (triplicate for each dilution), and CFUs were calculated based on the formula CFUs/disc = CFUs counted × dilution factor × 100. Statistical analysis was done using Student's *t*-test.

■ ASSOCIATED CONTENT

Ⓢ Supporting Information

NMR spectra (^1H, ^{13}C NMR, DEPT, HMQC, HMBC, and NOESY) for reported compounds are provided. This material is available free of charge via the Internet at http://pubs.acs.org.

■ AUTHOR INFORMATION

Corresponding Author

*Tel: +1 (806) 742-3062. Fax: +1 (806) 742-1289. E-mail: Paul.Pare@ttu.edu.

Notes

The authors declare no competing financial interest.

■ ACKNOWLEDGMENTS

This research was supported in part by the Robert Welch Foundation (D-1478), NSF equipment grant CHE-1048553, and NSF CRIF program.

■ REFERENCES

(1) Viuda-Martos, M.; Ruiz-Navajas, Y.; Fernandez-Lopez, J.; Perez-Alvarez, J. A. *J. Food Saf.* **2007**, *27*, 91−101.

(2) Piozzi, F. *Heterocycles* **1994**, *37*, 603−626.

(3) Piozzi, F.; Bruno, M.; Rosselli, S.; Maggio, A. *Heterocycles* **2005**, *65*, 1221−1234.

(4) Ulubelen, A.; Topcu, G.; Sonmez, U. *Stud. Nat. Prod. Chem.* **2000**, *23*, 591−648.

(5) Moustapha, C.; Hasen, T.; Waleed, M.; Sadaka, M. *Jordan J. Chem.* **2011**, *6*, 339−345.

(6) Belmekki, N.; Bendimerad, N.; Bekhechi, C.; Fernandez, X. *J. Med. Plants Res.* **2013**, *7*, 897−902.

(7) Nematollahi-Mahani, S. N.; Rezazadeh-Kermani, M.; Mehrabani, M.; Nakhaee, N. *Pharm. Biol.* **2007**, *45*, 295−298.

(8) De Marino, S.; Festa, C.; Zollo, F.; Incollingo, F.; Raimo, G.; Evangelista, G.; Iorizzi, M. *Food Chem.* **2012**, *133*, 21−28.

(9) Kamel, A. *J. Nat. Prod.* **1995**, *58*, 428−431.

(10) Djabou, N.; Lorenzi, V.; Guinoiseau, E.; Andreani, S.; Giuliani, M.-C.; Desjobert, J.-M.; Bolla, J.-M.; Costa, J.; Berti, L.; Luciani, A.; Muselli, A. *Food Control* **2013**, *30*, 354−363.
(11) Autore, G.; Capasso, F.; De, F. R.; Fasulo, M. P.; Lembo, M.; Mascolo, N.; Menghini, A. *Pharmacol. Res. Commun.* **1984**, *16*, 21−29.
(12) Otto, M. *Curr. Top. Microbiol. Immunol.* **2008**, *322*, 207−228.
(13) Parsek, M. R.; Singh, P. K. *Annu. Rev. Microbiol.* **2003**, *57*, 677−701.
(14) Costerton, J. W.; Stewart, P. S.; Greenberg, E. P. *Science* **1999**, *284*, 1318−1322.
(15) Periasamy, S.; Joo, H.-S.; Duong, A. C.; Bach, T.-H. L.; Tan, V. Y.; Chatterjee, S. S.; Cheung, G. Y. C.; Otto, M. *Proc. Natl. Acad. Sci. U.S.A.* **2012**, *109*, 1281−1286.
(16) Tran, P. L.; Lowry, N.; Campbell, T.; Reid, T. W.; Webster, D. R.; Tobin, E.; Aslani, A.; Mosley, T.; Dertien, J.; Colmer-Hamood, J. A.; Hamood, A. N. *Antimicrob. Agents Chemother.* **2012**, *56*, 972−978.
(17) Cho, K. J.; Jin, S.; Cui, J.; Yoon, T. R.; Ryu, P. Y. *J. Bacteriol. Virol.* **2008**, *38*, 197−205.
(18) Aslam, S. *Am. J. Infect. Control* **2008**, *36*, S175.e9−S175.e11.
(19) Tran, P. L.; Hammond, A. A.; Mosley, T.; Cortez, J.; Gray, T.; Colmer-Hamood, J. A.; Shashtri, M.; Spallholz, J. E.; Hamood, A. N.; Reid, T. W. *Appl. Environ. Microbiol.* **2009**, *75*, 3586−3592.
(20) Malone, C. L.; Boles, B. R.; Lauderdale, K. J.; Thoendel, M.; Kavanaugh, J. S.; Horswill, A. R. *J. Microbiol. Methods* **2009**, *77*, 251−260.
(21) Elmasri, W. A.; Hegazy, M.-E. F.; Aziz, M.; Koksal, E.; Amor, W.; Mechref, Y.; Hamood, A. N.; Cordes, D. B.; Pare, P. W. *Phytochemistry* **2014**, *103*, 107−113.
(22) Li, C.-M.; Zhang, X.-L.; Xue, X.-Y.; Zhang, F.-F.; Xu, Q.; Liang, X.-M. *Rapid Commun. Mass Spectrom.* **2008**, *22*, 1941−1954.
(23) Lu, C.-C.; Wang, J.-H.; Fang, D.-M.; Wu, Z.-J. *Rapid Commun. Mass Spectrom.* **2013**, *27*, 503−506.
(24) Yang, J.-H.; Kondratyuk, T. P.; Jermihov, K. C.; Marler, L. E.; Qiu, X.; Choi, Y.; Cao, H.; Yu, R.; Sturdy, M.; Huang, R.; Liu, Y.; Wang, L.-Q.; Mesecar, A. D.; van Breemen, R. B.; Pezzuto, J. M.; Fong, H. H. S.; Chen, Y.-G.; Zhang, H.-J. *J. Nat. Prod.* **2011**, *74*, 129−136.
(25) Agrawal, P. K. *Phytochemistry* **1992**, *31*, 3307−3330.
(26) Bianco, A.; Mazzci, R. A.; Melchioni, C.; Romeo, G.; Scarpati, M. L.; Soriero, A.; Uccella, N. *Food Chem.* **1998**, *63*, 461−464.
(27) Handjieva, N. V.; Ilieva, E. I.; Spassov, S. L.; Popov, S. S. *Tetrahedron* **1993**, *49*, 9261−9266.
(28) Ruhdorfer, J.; Rimpler, H. *Tetrahedron Lett.* **1981**, *22*, 839−842.
(29) Xie, H.; Morikawa, T.; Matsuda, H.; Nakamura, S.; Muraoka, O.; Yoshikawa, M. *Chem. Pharm. Bull.* **2006**, *54*, 669−675.
(30) Gilbert, K. *Plant Growth Regul.* **2001**, *34*, 149.
(31) Es-Safi, N.-E.; Kerhoas, L.; Ducrot, P.-H. *Rapid Commun. Mass Spectrom.* **2007**, *21*, 1165−1175.
(32) Neilson, E. H.; Goodger, J. Q. D.; Motawia, M. S.; Bjarnholt, N.; Frisch, T.; Olsen, C. E.; Moller, B. L.; Woodrow, I. E. *Phytochemistry* **2011**, *72*, 2325−2334.
(33) Morita, N.; Shimizu, M.; Arisawa, M. *Phytochemistry* **1973**, *12*, 421−423.
(34) Maruhenda, E.; Alarcon, D. L. L. C.; Garcia, M. D.; Cert, A. *Ann. Pharm. Fr.* **1987**, *45*, 467−470.
(35) Abdalla, S. S.; Abu, Z. M. H. *Planta Med.* **1987**, *53*, 322−324.
(36) Ulubelen, A.; Miski, M.; Neuman, P.; Mabry, T. J. *J. Nat. Prod.* **1979**, *42*, 261−263.
(37) Whang, W.-K. *Arch. Pharmacal Res.* **1994**, *17*, 5−10.
(38) Hirai, N.; Okamoto, M.; Udagawa, H.; Yamamuro, M.; Kato, M.; Koshimizu, K. *Biosci. Biotechnol. Biochem.* **1994**, *58*, 1679−1684.
(39) Machida, K.; Sakamoto, S.; Kikuchi, M. *J. Nat. Med.* **2009**, *63*, 227−231.
(40) Ruhdorfer, J.; Rimpler, H. *Z. Naturforsch., C: Biosci.* **1981**, *36C*, 697−707.
(41) Hammond, A. A.; Miller, K. G.; Kruczek, C. J.; Dertien, J.; Colmer-Hamood, J. A.; Griswold, J. A.; Horswill, A. R.; Hamood, A. N. *Burns* **2011**, *37*, 312−321.
(42) Cushnie, T. P. T.; Lamb, A. J. *Int. J. Antimicrob. Agents* **2005**, *26*, 343−356.
(43) Wang, H.; Sun, Y.; Ye, W. C.; Xiong, F.; Wu, H. J.; Yang, C. H.; Zhao, S. X. *Chem. Pharm. Bull.* **2004**, *52*, 615−617.